Journal of Nanoscience and Nanoengineering
Vol. 7, No. 1, 2021, pp. 1-9
http://www.aiscience.org/journal/jnn
ISSN: 2471-8378 (Print); ISSN: 2471-8394 (Online)

Photocatalytic Performance of Ca Doped ZnO Nanostructure Synthesized Via UV Incubator Shaker

Esraa Abdala[1], Omer Nur[2], Mustafa Abbas Mustafa[3, *]

[1]Department of Chemical Engineering, University of Khartoum, Khartoum, Sudan
[2]Department of Science and Technology, Campus Norrköping, Linkoping University, Norrköping, Sweden
[3]Materials and Nanotechnology Research Centre, University of Khartoum, Khartoum, Sudan

Abstract

The ZnO nanostructures were synthesized and doped with different concentrations of Ca (0.01, 0.03, 0.05 M) via the co-precipitation method using an incubator shaker with UV light at a temperature of 45°C and at 200 rpm. The precursors used were $Zn(NO_3)_2{\cdot}6H_2O$, $Ca(NO_3)_2{\cdot}4H_2O$ and NaOH. The morphological and structural properties were investigated by using different characterization techniques including X-ray diffraction (XRD), Fourier transform infrared spectroscopy (FT-IR), scanning electron microscope (SEM), energy dispersive spectra (EDS) and UV-visible spectroscopy. The average crystallite sizes of the samples were calculated by using the Debye-Scherrer's formula and were found to be in the nanorange. SEM images revealed that using UV light leads to the formation of high crystalline nanorods while non exposed UV light samples formed nanoparticles with less crystallinity. EDS shows that the synthetic route followed produced highly pure ZnO nanostructures. Finally the prepared samples were used as a photocatalyst to remove the Methylene blue (MB) dye. Observations showed that samples prepared without UV light have a smaller band gap and better photocatalytic degradation of Methylene blue compared to the UV light samples. The degradation of the MB dye achieved was 86.5 % and 96.93% for CZO_{UV} and CZO_{NUV} respectively following 10 min of treatment.

Keywords

Calcium Doping, MB Degradation, UV Light, Co-precipitation

Received: May 26, 2021 / Accepted: July 22, 2021 / Published online: July 26, 2021

1. Introduction

Nowadays, nanomaterials have attracted extensive interest in modern chemistry because of their unique superior properties for optical, electronic, magnetic and catalytic effects [1]. The properties of nanoparticles, which are different from the bulk, have encouraged many researchers to investigate nano-sized materials for their various applications [2]. Among the different nanomaterials, zinc oxide nanoparticles (ZnO NPs) present a promising candidate due to its properties such as being synthesized by cheap preparation methods, are nontoxic, and are a semiconductor. It has a wide direct band gap (3.37 eV) and large exciton binding energy (60 meV) at room temperature. There are a number of different applications such as gas sensors, chemical and biosensors, photo-photocatalysis, cosmetics, optical and electrical devices, drug-delivery and solar cells [3]. Many methods have been described in the literature for the synthesis of ZnO nanostructures such as laser ablation, hydrothermal methods [4], electrochemical depositions, sol–gel method, chemical vapor deposition and thermal decomposition. Recently, ZnO nanoparticles were prepared by ultrasound, microwave-

* Corresponding author
E-mail address: Dr.Mustafa.Abbas@gmail.com (M. A. Mustafa)

assisted combustion method, two-step mechanochemical-thermal synthesis, co-precipitation, and electrophoretic deposition [5]. Different morphologies of ZnO nanostructures were deomnstrated such as nanoparticles, nanowires, nanotubes, nanorods, and other complex morphologies from various synthetic methods [3].

Zinc and Titanium oxide have drawn much attention with regard to the degradation of various pollutants due to their high photosensitivity to UV light. However, ZnO is considered as a low cost alternative photocatalyst to TiO_2 for degradation of organics in aqueous solutions [6]. In a photocatalytic system, photo-induced reaction occurs at the surface of the catalyst. The excited electrons from the valence band jump to the conduction band thus generating an electron–hole pair. When a photocatalyst is illuminated by sufficiently energetic light stronger than its band gap energy, electron–hole pairs can migrate to the surface of the photocatalyst and participates in the chemical reaction. A redox reaction is initiated with water and oxygen and degradation of organic molecules absorbed on the surface of the photocatalyst occurs [7, 8]. On the contrary, ZnO exhibits low photocatalytic efficiency under visible light illumination. In order to utilize solar radiation more effectively, the development of a wide band gap ZnO is necessary to obtain different properties and applications. Thus efforts have been made to modify the optical properties, through shifting the optical absorption towards the visible region, through combining ZnO with other semiconductors in addition to doping ZnO.

Recent efforts have focused on the photocatalytic activity improvement of ZnO by tailoring its structure, including morphology, surface defects, and oxygen vacancies [9]. Jang et al. [7] prepared different ZnO photocatalysts morphologies using flame spray pyrolysis for the photocatalytic degradation of methylene blue in water. They reported 99% degradation after 1 hour with complete degradation after two hours. Shen et al. [6] deposited zinc oxide on the surface of silica nanoparticles using starch gel. The ZnO–Si exhibited higher photocatalytic activity as a result of the smaller particle size in combination with the better dispersion. The composite resulted in a 90% decomposition of methylene blue in an hour.

Alkaline earth metal elements can be taken as the candidate dopants to regulating and controlling the photo- catalytic properties, for example Yousefi et al. [8] used simple sol–gel to synthesize ZnO NPs with a narrow size distribution that was doped by Strontium with different concentrations to remove methylene blue (MB). It was observed that about 50% of MB was degraded within 45 and 30 min and it while it took 60 min at higher concentration to bleach the same quantity of MB. A great deal of work has been reported on Ca-doped ZnO (CZO), which possesses attractive properties for potential applications [10-12] but few that addressed its effect on band gap tailoring and photocatalytic degradation of Methylene blue. Srivastava et al. [13] briefed the effect of doping concentration of Ca in ZnCaO thin films and observed an increase in the band gap with Ca concentration increase. (Slama et al. [14] reported that it is possible to improve the efficiency of ZnO in the photocatalytic degradation of MB by doping with Ca^{2+} ions.

Zinc oxide has been prepared through various synthetic routes. Even though few have used UV light during synthesis, Wu and Chen [15] prepared ZnO nanowires by thermal decomposition assisted by UV-light and without UV light to study their photocatalytic properties and UV sensing. Comparatively Praus et al. [16] studied the ZnO precipitation under UV irradiation and the formation of oxygen vacancies. To the best of our knowledge no research was conducted to study the UV light during the synthesis of Ca doped ZnO and equally important no research reported using an incubator shaker for the synthesis of nanomaterials.

In the present investigation, we study co-precipitation synthesize of zinc oxide doped with different concentration of calcium at low temperature under ultraviolet-light making use of an incubator shaker since it provides high controlled environment within short time and without the use of organic solvents. Furthermore we investigate it's the synthesis route effect towards its band gap and photocatalytic activity by decomposition of methylene blue. For comparison purposes, we report the use of non UV light to observe the influence of the UV light on the morphology and UV absorbance of ZnO.

2. Experimental Methods

2.1. Synthesis of Ca Doped Zinc Oxide

All chemicals used in the experiment are of high purity (99.9 %) and purchased from Sigma Aldrich. For a typical calcium doped zinc oxide preparation, different concentrations of the Ca $(NO_3)_2{\cdot}4H_2O$ were completely dissolved in deionized water with $Zn(NO_3)_2{\cdot}6H_2O$. The prepared solution was then mixed with an aqueous solution of NaOH by adding simultaneously both solutions very slowly and a white gel was formed immediately. Followed by a vigorous stirring at ambient temperature for 15 min to achieve complete dissolution, the pH of the solution is maintained between 12 and 11. The former mixture is then agitated at 200 rpm in UV incubator shaker (Lab-Therm) under UV Light irradiation for 2 hrs at 45°*C*. Then the precipitate formed was washed 5 times with deionized water followed by centrifugation and was dried in hot air oven at 120°C for 2 hrs. Calcination was carried out at 600, 700 and

800℃ for 2 h. Samples obtained at different concentration ZnO: CaO (1: 0.01, 1: 0.03, 1: 0.05) and with UV and without UV identified as CZO_{UV} and CZO_{NUV} respectively.

2.2. Characterization Technique

The obtained powders of ZnO doped CaO nanoparticles (precursor), calcined at different temperatures, prior to synthesis under different light source were characterized by X-ray diffraction (XRD) using a SHIMADZU (XRD 6000 model) instrument with Cu- Ka radiation (l ¼ 1.5418 Å) in the 2θ range from 5 to 85 degrees with 0.02 increments. The peaks in the XRD patterns were indexed using ICDD 36e1451. Scherrer's equation Eq. (1) [15] was employed for the precise calculation of the average crystallite size using the full width at half maximum (FWHM) of the most intense peak.

$$D = \frac{0.89\lambda}{\beta cos\theta} \quad (1)$$

Where *D* is the crystallite size, 0.89 is Debye-Scherrer constant, λ represent the X-ray wavelength used;, β is the full line width at the half-maximum height of the main intensity peak, and θ is the Bragg angle. The lattice parameters *a* and *c* of the pure and Ca-doped ZnO samples were calculated from) oriented XRD peaks using eqs (2) and (3) [17].

$$a = \frac{\lambda}{\sqrt{3}sin\theta} \quad (2)$$

$$c = \frac{\lambda}{sin\theta} \quad (3)$$

The surface morphologies and size distribution of the agglomerates of the obtained samples was observed using an ultra-high-resolution scanning electron microscope (HRSEM, Hitachi S4100). The purity of the sample was tested by energy dispersive spectroscopy (EDS). The FT-IR spectra of the samples were recorded in the wavenumber region of 4000–400 cm^{-1} with a Shimadzu FT-IR spectrometer.

The UV–vis absorption spectra of the samples were recorded in the wavelength range of 200 to 800 nm at room Temperature using a Shimadzu UV 3600 to study the optical band gap properties of the calcium doped ZnO samples and determining the absorption using Gaussian function. The energy band gap (Eg) calculations were calculated using plotted Tauc plots between (αhʊ)2 and photon energy hʊ where α is the absorption coefficient of the material, λ is the wavelength, h is the Planck's constant, ʊ is the frequency of light and Eg is the band gap energy. The plotted graph plotted extrapolating the linear part of the graph until it meets the x-axis will give the value of the band gap. The Photocatalytic activity of the Ca doped ZnO were analyzed by monitoring the photo degradation of Methylene blue (MB) under sunlight irradiation using UV-Vis spectrophotometer Shimadzu-2101 UV/vis.

3. Results and Discussion

Characterization of Ca doped ZnO:

3.1. X-Ray Diffraction

Figure 1 depicted the XRD profiles of the CZO_{UV} calcined under various temperatures (600, 700, and 800°C) and at different concentrations ZnO: CaO (1: 0.01, 0.03, and 0.05). All samples showed a high crystalline nature and all the diffraction peaks are well indexed to the hexagonal ZnO wurtzite structure (JCPDS no. 36–1451). The crystallinity of the nanoparticles increases with the calcination temperature as it can be seen from the intensity of the peaks in Figure 1, (A). Diffraction peaks corresponding to the impurity were not found in the XRD patterns, confirming the high purity of the synthesized products.

At lower concentration of calcium (0.01 M) and low calcinations temperature (600°C), $CaCO_3$ peaks were detected and it was not shown at high calcination temperature (800°C). This can be attributed to the thermal decomposition of calcium carbonate to form CaO and CaOH. As expected presence of few peaks of calcium were observed at lower concentrations, suggesting it couldn't be detected by XRD measurements as confirmed by Dhahri et al. [18]. At higher concentration of the calcium dopant a justified peaks of calcium with a presence of CaO and Ca $(OH)_2$ has been shown. This behavior, already observed for calcium doped ZnO (Malpani, Varma and Mondal, 2016), which could be a result from the conversion of some CaO into $Ca(OH)_2$ when it exposed to the atmosphere. From XRD Data Figure 2, as the Ca content increased (0.01, 0.03, and 0.05) a slight shift of the XRD peaks towards higher 2-theta degrees is observed indicates a local distortion of the wurtzite lattice, which in inconsistent with the result obtained by (Dhahri *et al. [18]* and Ghiloufi *et al.* [19] due to the differences in the ion sizes between, zinc (1.42 Å) and calcium (1.94 Å) which lead to some residual stress inside the nanoparticles. Nevertheless when increasing calcination temperature, a shift of peaks 2-theta degrees (not shown) is observed. The effect of the light source is shown in the XRD data Figure 2 as the crystallinity of the CZO_{UV} nanoparticles is superior to that of the ZnO_{NUV} at different concentrations of Ca dopant confirming that UV light acts as important growth factor. From Scherrer's equation (eq. 1) the average crystallite size varying in the range 25–38 nm, it increases with the increase in calcination temperature, the similar trend has also observed in literature [20] and slightly with increasing calcium loading.

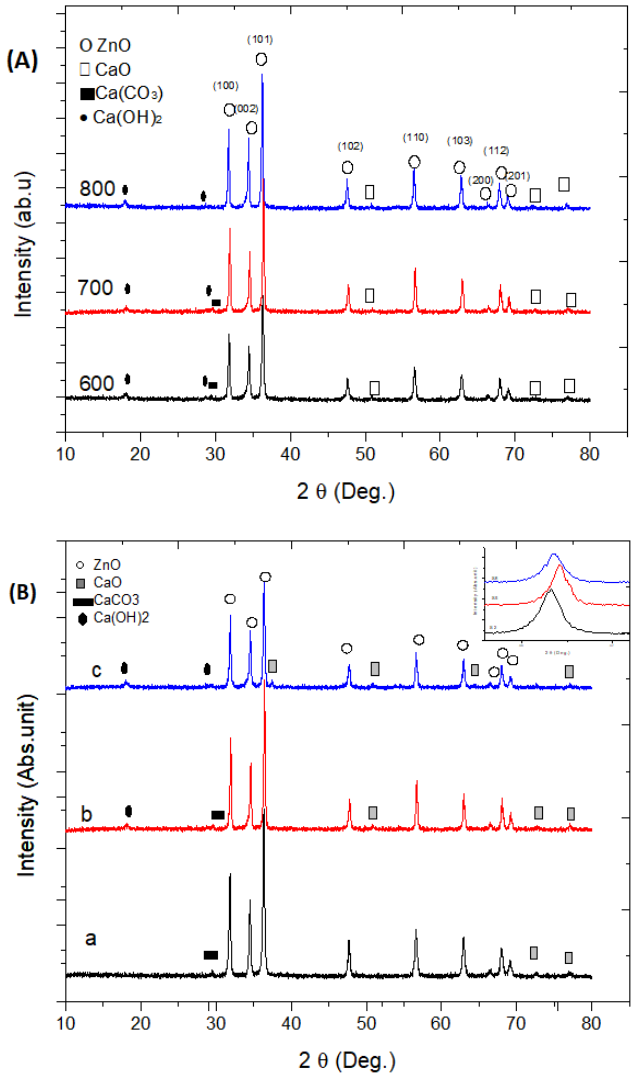

Figure 1. XRD profile of CZO_{UV} (A) 0.03 M of CZO calcined at different temperature (B) Different concentration of CZO_{UV} calcined at 700°C (a) 0.01 CZO_{UV} (b) 0.03 CZO (c) 0.05 CZO_{UV}.

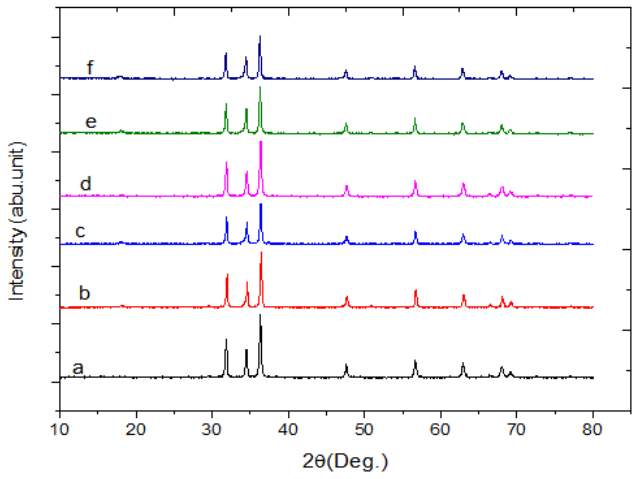

Figure 2. XRD profile of CZO_{UV} at 700°C (a) 0.01 M CZO_{UV} (b) 0.03 M CZO_{UV} (c) 0.05 M CZO_{UV}, and CZO_{NUV} calcined at 700°C (d) 0.01 CZO_{NUV} (e) 0.03 CZO_{NUV} (f) 0.05 CZO_{NUV}.

The lattice parameters deviation is caused by the presence of various point defects [21]. Table 1 shows the effect of calcination temperature on lattice parameters for CZO_{UV} and CZO_{NUV} as it expands with increase in temperature [22] and surprisingly it's noticed that the lattice decreases again at high temperature 800°C. Also an increase of *c* axis was observed for the doped samples which are attributed to the inclusion of calcium into the Zn sites as the c axis has the fastest growth direction [23]. Figure 3 illustrates the calculated lattice parameters for CZO_{UV} for 0.03 concentration of Ca doped ZnO.

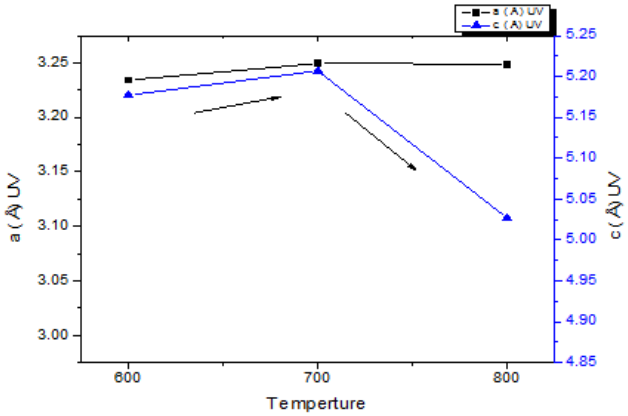

Figure 3. Trend of lattice parameters (a, c) for 0.03 M CZO_{UV} at different calcination Temperature.

3.2. SEM Characterization

The HRSEM analysis showed completely different morphologies based on the condition of the reaction such as light source used during synthesis, calcination temperature and the concentration of calcium doped in zinc. It was observed that the nanoparticles form a flower like structure. The average diameter of these self-oriented flowers like structures is 250–300 nm, in very less quantity a secondary morphology like plates and agglomerated particles were also observed.

Figure 4 reveals that using UV light plays a dominant factor for the formation of nano rods morphology while a nanoparticle was obtained in non UV light. The SEM images reflect that an increase in calcination temperature for nanoparticles prepared under UV light from 600°C to 700°C shows increase in the width of nanorods and slight decrease in the length, then the nanorods diffuses into each other forming a glassy phase. Calcination at higher temperature (800°C) significantly causes the morphological changes from rods to spherical shape and also it causes increase in the particle size, agglomeration of CaO and ZnO clusters are due to sintering effect as agreed with literature [2, 24] ZnO nanoparticles prepared using none UV light have particle like morphology and obviously shows that ZnO nanoparticles form larger nanoparticles with increase in calcination temperature (not shown). The effect of the calcination temperature was seen in the colour of the synthesized sample

as it was white before calcination and it changed to yellow after it was exposed to 600℃ calcination temperature and slightly yellow at 700℃ to white at 800℃ confirm the result obtained and by Udayabhaskar et al. [11].

Table 1. Variation of lattice parameters with calcination temperature.

		hkl (101)		Lattice Parameters		
Sample	**Temperature**	**2θ**	**D**	**a (Å)**	**c (Å)**	**c/a**
CZO_{UV} 0.03	600	36.54	33.94651	3.2342	5.1772	1.600767
CZO_{UV} 0.03	700	36.35	43.62169	3.2495	5.2069	1.60237
CZO_{UV} 0.03	800	36.37	38.17117	3.249	5.0270	1.547245
CZO_{UV} 0.05	600	36.37	30.53693	3.2342	5.1772	1.600767
CZO_{UV} 0.05	700	36.16	33.90957	3.2533	5.2073	1.600621
CZO_{UV} 0.05	800	36.37	38.17117	3.2495	5.2069	1.60237
CZO_{NUV} 0.03	600	36.63	27.78163	3.2342	5.1772	1.600767
CZO_{NUV} 0.03	700	36.17	38.14935	3.2533	5.2073	1.600621
CZO_{NUV} 0.03	800	36.34	33.92701	3.2495	5.2069	1.60237
Standard ZnO	-	36.253	-	3.249	5.2060	1.602239

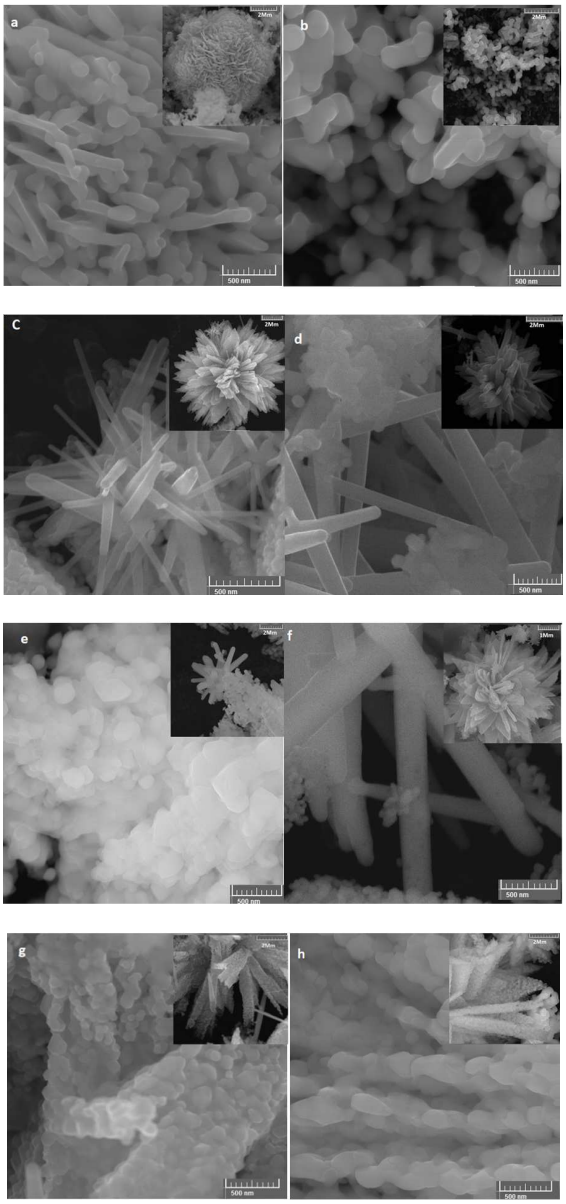

Figure 4. SEM images (a) Pure ZnOUV (b) Pure ZnONUV control Calcined at 700°C, (c, d, e) Zn: Ca ratio 1: 0.03 CZNUV calcined at 600, 700, 800°C respectively (f, g, h) Zn: Ca ratio 1: 0.05 CZNUV calcined at 600, 700, 800°C respectively.

The energy dispersive spectra of the samples obtained from the SEM-EDS analysis (Figure 5) clearly show that the sample prepared by the above route has the presence of the main elements Zn, O and Ca dopant and their distribution of all and each element with oxygen in different spectrums.

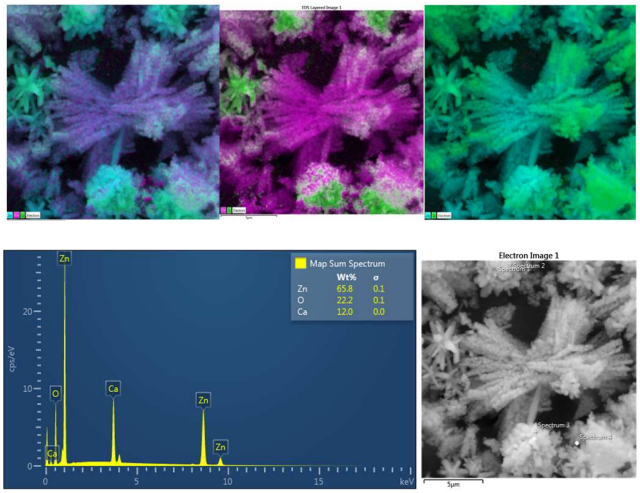

Figure 5. EDS spectrum for 0.03 M of $CaZO_{UV}$ Calcined at 600°C.

3.3. FTIR Characterization

The FTIR spectrum $CaZnO_{UV}$ nanoparticles and for pure ZnO at different calcination temperatures are shown in Figure 6. The peaks correlated to crystalline metal oxide bond (ZnO) observed at 420-480 cm^{-1} purity of the samples were obvious in Figure 6 an obvious peak correlated for O-H is shown in low calcination temperature 600°C. In the FTIR spectra Figure 6 for $CaZnO_{UV}$ with 0.05 calcium concentration we can observe that in the higher calcination temperature a less absorption of CO_3^{2-}, confirming the result obtained by XRD. The absorption peaks of O-H from 3200-3643 cm^{-1} resulted from water molecule adsorption [1, 25].

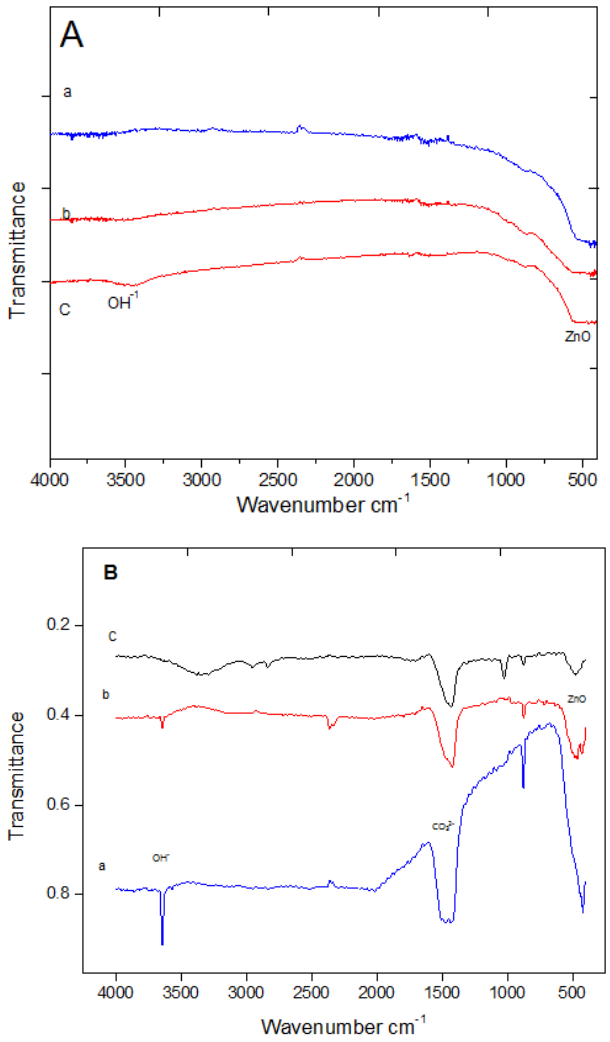

Figure 6. FTIR spectrum (A) ZnO Control at (a) 600°C (b) 700°C (c) 800°C, (B) CaZnOUV (0.05) at (a) 600°C (b) 700°C (c) 800°C.

3.4. UV Visible Study

Figure 7 shows The UV visible absorption spectra of the CZO 0.03 M samples after calcination at 600, 700 and 800°C for UV and NUV samples using Gaussian fitting function. The figure demonstrates strong absorption peaks for CZO 0.03 M at different calcination temperatures at wavelength between (441-442) nm and (450-454) nm for UV and NUV samples respectively. These shifts towards the higher energy wavelength of light imply band gap narrowing as confirmed by the analysis of the spectroscopic data via Tauc plots. Figure 8 showing the energy band gap when using different concentration of calcium doping 0.01, 0.02, 0.03 M calcined at 700℃. Clearly following the synthesis route of co-precipitation in incubator shaker decreases the band gap for nanocrystals of undoped zinc oxide ZnO_{UV} (2.937 eV) and ZnO_{NUV} (2.136 eV) where both are less than that of the bulk (3.37 eV) the reason can be mainly due to the downward shifts of the conduction band due to lattice contraction in nanoparticles as a result of high attractive electrostatic interaction between Zn^{2+} and O^{2-} ions as crystallinity of the samples plays a very important part in the band gap change of materials [26, 27].

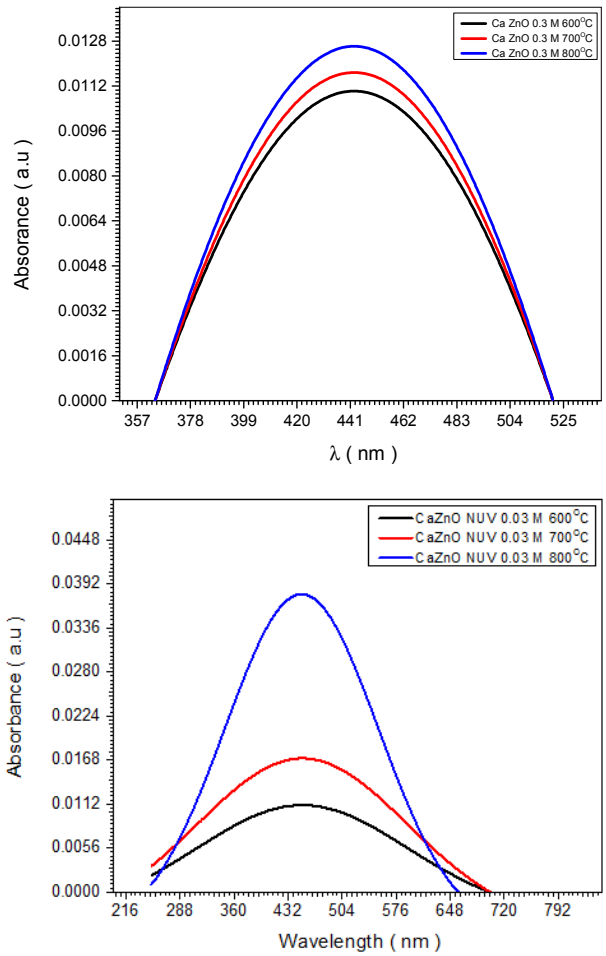

Figure 7. UV visible spectra for CZO_{UV} calcium concentration (0.03) at (a) 600°C (b) 700°C (c) 800°C.

Considerable reduction in the band gap of CZO_{NUV} samples is noticed more than CZO_{UV} this can be attributed to using NUV increases the active defect sites generated in ZnO lattice by Ca ions. As a result, more visible-light is absorbed via these active defect sites, which may lead to a more photocatalytic activity of the doped $CZnO_{NUV}$ crystallites in visible-light regions. For example, at a calcination temperature of 700°C when using UV light, undoped ZnO has a band gap value of 2.937 eV, and it increases with Ca 0.01 but it decreased with increasing Ca content whereas the band gaps are 2.919, 2.988, 2.983 for 0.01, 0.03, 0.05 respectively. For NUV the undoped ZnO has a band gap 2.136 and its decreasing with calcium doping surprisingly the narrowest band gap was for 0.03 M which reached 1.963 and an increase for 0.05 M to 2.536 this phenomenon could be due to particle size effects on band gap of the nanostructures this similar phenomenon also observed by Yousefi et al. [8].

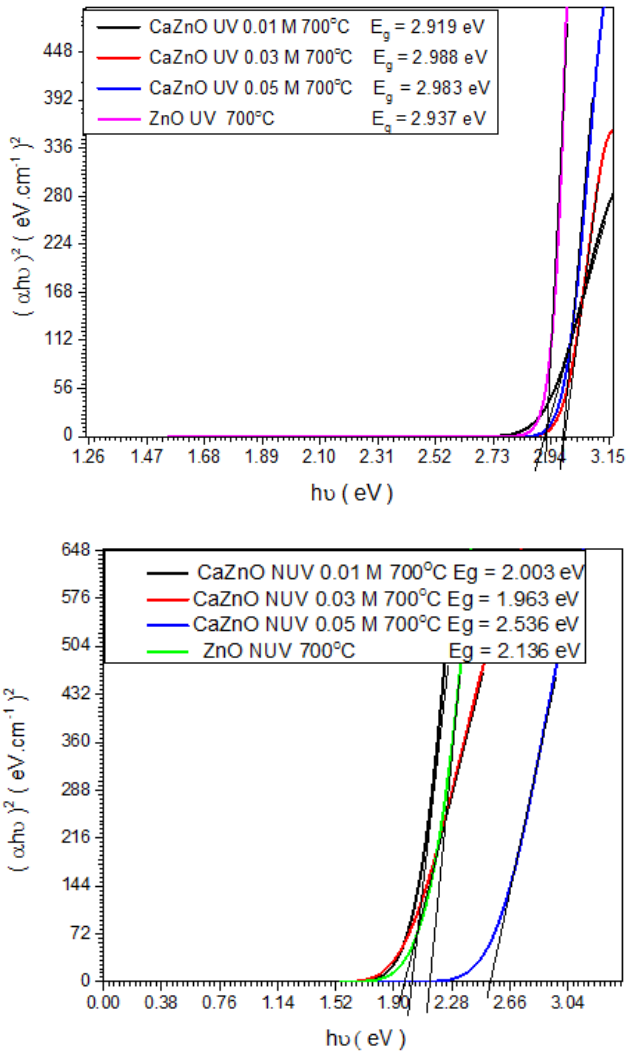

Figure 8. Band gap for CZO_{UV} and CZO_{NUV} calcined at 700°C different calcium concentration 0.01, 0.03 and 0.05.

3.5. Photocatalytic Degradation for Methylene Blue

The prepared samples were examined as photocatalysts for the degradation of methylene blue under sunlight. Under a typical experiment 0.06 g of the sample was stirred for 15 min with (50 mL of 1 × 10^{-5} M) aqueous solution of methylene blue then kept under dark for 30 min followed by stirring under sunlight irradiation for 10 min. Aliquot was taken out at equal time intervals, and the absorption spectra were recorded at λ_{max} =665 nm using UV-Vis spectrophotometer then the percentage of degradation was calculated and the photocatalytic rate constant for methylene blue degradation (k) was determined from the first-order plot using eq (4).

$$\ln(\frac{A_0}{A}) = kt \quad (4)$$

Where A_0 is the initial absorbance, A is the absorbance after a time t, and k is the first-order rate constant [17, 28].

Figure 9 illustrates the MB degradation for samples calcined at 700℃ using same content of doped calcium, significantly higher photocatalytic activities of Ca doped ZnO can be seen. CZO_{NUV} has a photocatalytic activity superior to $CZnO_{UV}$ and it can be explained by their decreased band gap values as obtained from UV results and from Figure 10 it can be seen than higher photocatlytic degradation achieved at calcination temperature 700℃ when using 0.01 M for CZO_{UV}. Table 2 showed that all samples exhibited a good absorption for MB for irradiation times of 0-10 min in equal intervals that can be due to the shift of the band gap to the visible region which obviously caused a higher redox potential of the photoexcited electron−hole pairs, beside the increase in the surface area where photocatalytic reactions mainly occur which significantly increases the activity of the photocatalyst. For examples when calcium content was 0.03 M, MB degradation achieved was 86.5% and 96.93% for CZO_{UV} and CZO_{NUV} respectively after 10 min and a complete MB degradation observed at 4 min and 1 min for CZO_{UV} and CZO_{NUV} respectively when increasing the calcium content to 0.05 M. From these results we can conclude that the degradation of MB is a function of the light used during synthesis and amount of calcium doped as a poor degradation noticed for undoped zinc oxide

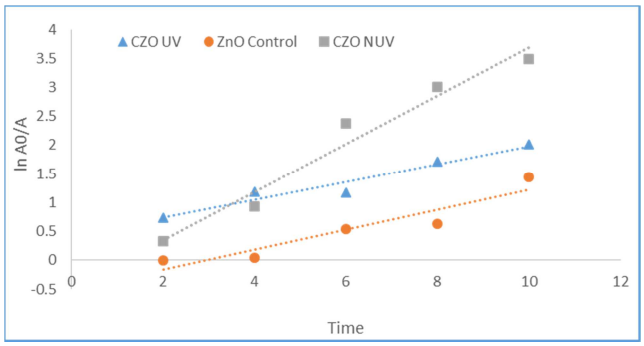

Figure 9. Photocatalytic MB degradation for samples calcined at 700°C ZnO control, CZO_{UV} 0.03, $CaZn_{NUV}$ 0.03.

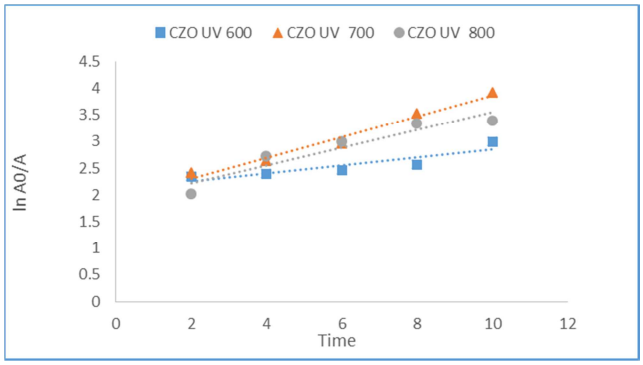

Figure 10. Photocatalytic MB degradation for samples CZn_{UV} 0.01 calcined at calcined at 600, 700, 800°C.

Table 2. Degradation % of MB at calcination temperature 700℃ for different concentrations of CaZnO.

Conc. of Calcium doped in ZnO (CZO)	Degradation %f MB at calcination temperature 700°C			
	CZO_{UV}	CZO_{NUV}	Undoped ZnO_{UV}	Undoped Zn_{NUV}
0.01	81.8%	92.9%		
0.03	86.5%	96.93%	76.22%	84.64%
0.05	100% after 4 min.	100% after 1 min.		

4. Conclusion

The use of an incubator shaker proved to be a simple and effective instrument for synthesizing Ca (0.01, 0.03, 0.05 M) doped ZnO (CZO) nanostructure by co-precipitation method, under different light sources UV and non UV and followed by calcination at temperatures ranging from 600 to 800 °C. The CZO samples containing lower Ca-content exists as pure wurtzite phase of ZnO in the XRD, whereas, crystals of cubic CaO secondary phase identified for 0.03 M and 0.05 M CZO. Moreover CZO particles exhibited smaller crystallite size and an increase in c/a ratio with increase in calcination temperature and concentration of Ca doped in Zn. The FTIR and XRD revealed that absorption of $CaCO_3$ decreased at higher calcination temperatures. SEM results showed that using UV light affect the nanostructure morphology as it results in the formation of nanorods while non UV light formed nanoparticles. All samples prepared by incubator shaker have strong absorption in the visible-light region and smaller band gaps. Though, CZO_{NUV} samples showed a better photocatalytic performance for degradation of MB than CZO_{UV} samples.

Acknowledgements

The authors are grateful for the financial support from the Osman Elbashir Research Grant (Prof. Nimir O. Elbashir, Texas A&M University, Qatar) under the Chemical Engineering Department at the University of Khartoum.

References

[1] Sadollahkhani, A., Kazeminezhad, I., *et al.* (2014) 'Synthesis, structural characterization and photocatalytic application of ZnO@ZnS core-shell nanoparticles', *RSC Advances*. Royal Society of Chemistry, 4 (70), pp. 36940–36950. doi: 10.1039/c4ra05247a.

[2] Raou, D. (2013) 'Synthesis and microstructural properties of ZnO nanoparticles prepared by precipitation method', 50, pp. 932–937. doi: 10.1016/j.renene.2012.08.076.

[3] Vaseem, M., Umar, A. and Hahn, Y. (1988) *ZnO Nanoparticles : Growth, Properties, and Applications*.

[4] Ni, Y. H. *et al.* (2005) 'Hydrothermal preparation and optical properties of ZnO nanorods', *Materials Science and Engineering B: Solid-State Materials for Advanced Technology*, 121 (1–2), pp. 42–47. doi: 10.1016/j.mseb.2005.02.065.

[5] Kumar, S. S., Venkateswarlu, P., Rao, V. R. and Rao, Gollapalli Nageswara (2013) 'Synthesis, characterization and optical properties of zinc oxide nanoparticles', *International Nano Letters*, 3 (1), p. 30. doi: 10.1186/2228-5326-3-30.

[6] Shen, W. *et al.* (2008) 'Photocatalytic degradation for methylene blue using zinc oxide prepared by codeposition and sol-gel methods', *Journal of Hazardous Materials*, 152 (1), pp. 172–175. doi: 10.1016/j.jhazmat.2007.06.082.

[7] Jang, Y. J., Simer, C. and Ohm, T. (2006) 'Comparison of zinc oxide nanoparticles and its nano-crystalline particles on the photocatalytic degradation of methylene blue', *Materials Research Bulletin*, 41 (1), pp. 67–77. doi: 10.1016/j.materresbull.2005.07.038.

[8] Yousefi, R. *et al.* (2015) 'Enhanced visible-light photocatalytic activity of strontium-doped zinc oxide nanoparticles', *Materials Science in Semiconductor Processing*, 32, pp. 152–159. doi: 10.1016/j.mssp.2015.01.013.

[9] Bai, X. *et al.* (2013) 'Performance enhancement of ZnO photocatalyst via synergic effect of surface oxygen defect and graphene hybridization', *Langmuir*, 29 (9), pp. 3097–3105. doi: 10.1021/la4001768.

[10] Water, W. and Yang, Y. S. (2006) 'The influence of calcium doped ZnO films on Love wave sensor characteristics', *Sensors and Actuators, A: Physical*, 127 (2), pp. 360–365. doi: 10.1016/j.sna.2005.12.023.

[11] Udayabhaskar, R., Mangalaraja, R. V. and Karthikeyan, B. (2013) 'Thermal annealing induced structural and optical properties of Ca doped ZnO nanoparticles', *Journal of Materials Science: Materials in Electronics*, 24 (9), pp. 3183–3188. doi: 10.1007/s10854-013-1225-z.

[12] Santangelo, S. *et al.* (2017) 'Effect of calcium- and/or aluminum-incorporation on morphological, structural and photoluminescence properties of electro-spun zinc oxide fibers', *Materials Research Bulletin*. Elsevier Ltd, 92, pp. 9–18. doi: 10.1016/j.materresbull.2017.03.062.

[13] Srivastava, A. *et al.* (2014) 'Blue-light luminescence enhancement and increased band gap from calcium- doped zinc oxide nanoparticle films Materials Science in Semiconductor Processing Blue-light luminescence enhancement and increased band gap from calcium-doped zinc oxide nanoparticl', *Materials Science in Semiconductor Processing*. Elsevier, 26 (December 2017), pp. 259–266. doi: 10.1016/j.mssp.2014.05.001.

[14] Slama, R. *et al.* (2016) 'Effect of Ca-doping on microstructure and photocatalytic activity of ZnO nanoparticles synthesized by sol gel method', *Journal of Materials Science: Materials in Electronics*. Springer US, 27 (8), pp. 7939–7946. doi: 10.1007/s10854-016-4786-9.

[15] Wu, J. M. and Chen, Y. R. (2011) 'Ultraviolet-light-assisted formation of ZnO nanowires in ambient air: Comparison of photoresponsive and photocatalytic activities in zinc hydroxide', *Journal of Physical Chemistry C*, 115 (5), pp. 2235–2243. doi: 10.1021/jp110320h.

[16] Praus, P., Tokarský, J. and Svoboda, L. (2015) 'Contribution to synthesis of ZnO nanoparticles by UV irradiation-assisted precipitation', *NANOCON 2015 - 7th International Conference on Nanomaterials - Research and Application, Conference Proceedings*.

[17] Vinodkumar Etacheri, Roshith Roshan, and V. K. (2014) 'Mg-Doped ZnO Nanoparticles for Efficient Mg-Doped ZnO Nanoparticles for E ffi cient Sunlight-Driven', (May 2012). doi: 10.1021/am300359h.

[18] Dhahri, R. *et al.* (2017) 'Sensors and Actuators B : Chemical Enhanced performance of novel calcium / aluminum co-doped zinc oxide for CO 2 sensors', *Sensors & Actuators: B. Chemical*. Elsevier B. V., 239, pp. 36–44. doi: 10.1016/j.snb.2016.07.155.

[19] Ghiloufi, I. *et al.* (2016) 'Preparation and characterization of Ca-doped zinc oxide nanoparticles for heavy metal removal from aqueous solution', *MRS Advances*, 1 (53), pp. 3607–3612. doi: 10.1557/adv.2016.511.

[20] Kumar, S. S., Venkateswarlu, P., Rao, V. R. and Rao, Gollapalli Nagewsara (2013) 'Synthesis, characterization and optical properties of zinc oxide nanoparticles', pp. 1–6.

[21] Ghosh, S. P. (2012) 'SYNTHESIS AND CHARACTERIZATION OF ZINC OXIDE NANOPARTICLES BY SOL-GEL PROCESS Synthesis and Characterization of Zinc Oxide Nanoparticles by Sol-Gel Process', *Master's Thesis*, (410). doi: ARTN 51\r10.1186/s12916-015-0290-y.

[22] Raoufi, D. (2013) 'Synthesis and microstructural properties of ZnO nanoparticles prepared by precipitation method', *Renewable Energy*, 50, pp. 932–937. doi: 10.1016/j.renene.2012.08.076.

[23] Greene, L. E. *et al.* (2005) 'General route to vertical ZnO nanowire arrays using textured ZnO seeds', *Nano Letters*, 5 (7), pp. 1231–1236. doi: 10.1021/nl050788p.

[24] Ngamcharussrivichai, C., Totarat, P. and Bunyakiat, K. (2008) 'Ca and Zn mixed oxide as a heterogeneous base catalyst for transesterification of palm kernel oil', *Applied Catalysis A: General*, 341 (1–2), pp. 77–85. doi: 10.1016/j.apcata.2008.02.020.

[25] Photocatalysis, S. (2014) 'Mg-Doped ZnO Nanoparticles for Efficient Mg-Doped ZnO Nanoparticles for E ffi cient Sunlight-Driven', (May 2012). doi: 10.1021/am300359h.

[26] Kamarulzaman, N., Kasim, M. F. and Rusdi, R. (2015) 'Band Gap Narrowing and Widening of ZnO Nanostructures and Doped Materials', *Nanoscale Research Letters*. Nanoscale Research Letters, 10 (1). doi: 10.1186/s11671-015-1034-9.

[27] Ions, K. M. *et al.* (2018) 'Defect Induced Band Gap narrowing of Zinc Oxide Nanoparticles using Li +, Defect Induced Band Gap narrowing of Zinc Oxide Nanoparticles using Li +, Na + and K + Metal Ions as a Dopant', (March).

[28] Shahabuddin, S., Sarih, N. M. and Mohamad, S. (2016) 'Nanocomposites with Enhanced Photocatalytic Degradation of Methylene Blue under Visible Light'. doi: 10.3390/polym8020027.